Clays and Clay Minerals, Vol. 68, No. 2:161–174, 2020

ANALYSIS OF THE MINERAL COMPOSITIONS OF SWELL-SHRINK CLAYS FROM GUANGXI PROVINCE, CHINA

ZHAOTIAN ZENG[1]*, HAIBO LU[1,2], YANLIN ZHAO[3]*, AND YINGHONG QIN[3]

[1]College of Civil and Architecture Engineering, Guilin University of Technology, Guilin 541004, China
[2]College of Civil Engineering, Hezhou University, Hezhou 542899, China
[3]College of Civil Engineering and Architecture, Guangxi University, Nanning 530004, China

Abstract—Swell-shrink clays are widely distributed in the Guangxi province of southern China in the form of expansive soils and lateritic clays. They have high particle dispersion, poor permeability, and significant swell-shrink properties. In recent decades, a series of problems closely related to the physical-mechanical properties of the swell-shrink clays have been encountered in various engineering projects. Mineral composition is a critical factor affecting the physical-mechanical properties of these clays. However, determining accurately their mineral compositions is difficult because the analytical methods available are expensive, time consuming, and have a high possibility of errors. Therefore, identifying a method suitable for quantitatively analyzing the mineral composition of the swell-shrink clays is necessary. In the current study several swell-shrink clays, including two expansive soils and four lateritic clays, from the Guangxi region were investigated. Qualitative analytical methods such as differential thermal analysis (DTA) and X-ray diffraction (XRD) were conducted to identify the mineral composition of the soils. The results indicated that the expansive soils were composed mainly of quartz (Qz), montmorillonite (Mnt), illite (Ilt), and kaolinite (Kln). The Baise specimen also contained a certain amount of calcite (Cal), while the lateritic clays primarily contained Kln and goethite (Gth) as well as lesser amounts of Qz and gibbsite (Gbs). On the basis of the aforementioned results, rough quantitative analyses of the mineral compositions were conducted using X-ray fluorescence (XRF) and the Bogue method. The results indicated that the lateritic clay samples from Wuming, Guilin, and Liuzhou contained 70–80% Kln, while the Laibin lateritic clay was 50% Kln. The lateritic clays contained ~10% Gth. The expansive soils were 30–40%, 25–30%, and 10–15% of Ilt, Qz, and Mnt, respectively. Finally, the relationships between the mineral compositions, zeta potentials, and free swelling ratios are discussed briefly. This investigation indicated that the zeta potential was mainly related to the type and content of clay minerals in the soil when neutral water was used as the free solution (pH = 7). The correlation between the swelling index and the zeta potential of the expansive soils was greater than that of the lateritic clays, which indicated that the swelling properties of expansive soils were more affected by the clay mineral composition than those of the lateritic clays. The results provide a systematic method for the qualitative and quantitative analysis of the mineral composition of swell-shrink clays and primary data for studying how mineral composition affects the physical properties of swell-shrink clays in the study area.

Keywords—Free swelling ratio · Mineral composition · Swell-shrink clay · Zeta potential

INTRODUCTION

Swell-shrink clays have high particle dispersion, poor water permeability, and significant swell-shrink properties (Tan and Kong 2006). This type of clay is distributed widely in the Guangxi province of southern China in the form of expansive soil and lateritic clay (Lu et al. 2013a, b). In the 1970s, a number of disasters occurred in expansive soil areas in China, resulting in large economic losses (Liao 1984; Li et al. 1997). For example, the Nanning–Kunming Railway contains a total of 60 km of expansive-soil subgrade, and 28 expansive soil subgrade disasters occurred between December 1997 and end 1999 (Feng et al. 2001). Engineering disasters related to lateritic clay, such as slope instability, differential foundation settlement, and dam cracking, have also occurred occasionally. In recent decades, extreme climatic variations have occurred frequently in China, resulting in hot and rainy weather. The above-mentioned engineering problems and geological disasters related to swell-shrink clays will become increasingly serious because their special expansion and contraction characteristics are related closely to their water content. Therefore, understanding fully the physical-mechanical characteristics of these swell-shrink clays is necessary (Sun et al. 2016).

Mineral composition greatly influences the physical-mechanical properties of soils (Mitchell and Soga 2005). As early as the 1950s, Norrish (1954, 1961) studied the expansion of montmorillonite (Mnt) crystals. Tan (1997) investigated the expansion and contraction mechanism of Mnt crystals and discussed the relationships among the crystal surface spacing of Mnt, the type of electrolyte solution, and electrolyte concentration. Shao et al. (1994) analyzed the mineral composition of expansive soils using XRD and DTA, and they explored the relationship between mineral composition and expansion characteristics. Their results indicated that the engineering properties of an expansive soil were affected significantly by its mineral composition. Tan and Kong (2001) also conducted a series of studies on the expansion and contraction of Mnt crystals and analyzed the causes of different expansion and contraction characteristics of unsaturated Mnt crystals. Wang (1983) studied the cementation of lateritic clays and discussed the influence of free iron oxide on their engineering properties. His results indicated that the mechanical properties of lateritic clays were close to those of normal clays once the free iron oxide was removed. Kong et al. (1995) further studied the cementation characteristics of a

* E-mail address of corresponding author: zengzhaotian@glut.edu.cn
DOI: 10.1007/s42860-019-00056-7

lateritic clay and found that only some of the free ferric oxide played a role in the cementation process. The aforementioned studies indicate that the mineral composition influences the physical and mechanical properties of swell-shrink clays due to the clay mineral and cementation materials.

For many years, studies have focused on the composition and microstructure of the minerals and cementation materials in swell-shrink clays (Arca and Weed 1966; Madu 1977; Luo 1983; Qu et al. 2002; Tan and Kong 2006; Lu et al. 2012). Some scholars have conducted in-depth studies on the quantitative analysis of mineral composition. For instance, Tan (1984) analyzed quantitatively the clay minerals in mixed samples of minerals using a simplified algorithm. Zhang and Fan (2003) suggested XRD as a simple, quick analytical method to determine quantitatively the material phases of clay minerals. Dai et al. (2005) used the diffraction strength and width at half height XRD values to analyze quantitatively the mineral compositions of expansive soils. However, the above-mentioned analytical methods are expensive, time consuming, and have significant possibility of errors which are rarely mentioned. Therefore, finding a suitable quantitative method to analyze the mineral composition of swell-shrink clays is essential.

Zeta potential is defined as the electrical potential developed at the solid–liquid interface in response to relative movement of soil particles and water (Derjaguin and Landau 1941; Verwey and Overbeek 1948; Van Olphen 1977; Sparks 1986; Yukselen-Aksoy and Kaya 2011). Zeta potential is one of the important electrokinetic properties of clay minerals and a good indicator of their electrical potentials: the higher the zeta potential, the greater the electrical potential of the clay particle (Derjaguin and Landau 1941; Verwey and Overbeek 1948; Van Olphen 1977; Erzin and Yukselen 2009; Farahani et al. 2019). Zeta potential could be considered as an index to assess the effect of surface charge of the particles on the status of soil dispersibility (Derjaguin and Landau 1941; Verwey and Overbeek 1948; Van Olphen 1977; Chorom and Rengasamy 1995). Measuring the electrophoretic mobility of clay particles and deriving zeta potential from the mobility give a measure of the net charge on the clay surface (Marchuk and Rengasamy 2011). Zeta potential has been recognized a very good index of the repulsive interaction between colloid particles. In addition, one may assume that zeta potential measures the potential related to the diffuse part of the double layer (Derjaguin and Landau 1941; Verwey and Overbeek 1948; Van Olphen 1977; Ofir et al. 2007). In fact, the diffuse double layer (DDL) is a critical factor in explaining the expansion properties of swell-shrink clays (Mitchell and Soga 2005). Therefore, discussion of the relations between the zeta potential, mineral compositions, and expansion properties is very important.

The purpose of the present study was to determine the relationships among zeta potential, mineral composition, and soil expansion properties in several swell-shrink clays, including two expansive soils and four lateritic clays, from the Guangxi region, using a series of qualitative and quantitative mineral composition analyses, such as DTA XRD, chemical element analysis, X-ray fluorescence (XRF), and the Bogue method, in order to provide primary data to explain the effect of mineral compositions on the physical properties of swell-shrink clays.

MATERIALS AND METHODS

Materials

The study area is located in Guangxi province, southern China, which is a subtropical monsoon climate area between 20°54' N and 26°24' N latitude. The annual rainfall is >1070 mm and the average annual temperature is 16.5–23.1°C. Through extensive investigation and comparison, two expansive soils and four lateritic clays were selected for the present study and collected from Nanning, Baise, Guilin, Liuzhou, Laibin, and Wuming (Fig. 1).

Undisturbed soil specimens were sampled and tested in the laboratory to determine basic soil properties such as the bulk density, moisture content, Atterberg limits, particle composition, free swelling ratio, linear/volumetric shrinkage ratio, shrinkage coefficient, and the shrinkage limit according to Specification of Soil Test (SL 237-1999, 1999). The results of these analyses (Tables 1 and 2) revealed that the six soils were high-plastic clays composed predominantly of < 0.002 mm colloid particles, except for the Wuming lateritic clay. The colloid particle contents (<0.002 mm) of Nanning, Baise, Guilin, Liuzhou, and Laibin samples were 57.36, 45.23, 53.50, 47.59, and 46.30%, respectively. The Wuming lateritic clay was composed of only 13.65% of < 0.002 mm colloid particles and contains numerous ferrous-manganese nodules and un-weathered parent rocks. The four lateritic clays had relatively low free swelling ratios (< 40%) (Table 2). The linear shrinkage ratios of the lateritic clays from Guilin, Liuzhou, and Laibin were 3–5%, while the ratio of the Wuming lateritic clay was 0.38%. The two expansive soils had relatively high free swelling ratios (>40%). The free swelling ratios of the Nanning

Fig. 1 Map showing sample locations.

https://doi.org/10.1007/s42860-019-00056-7 Published online by Cambridge University Press

Table 1 Basic physical properties of the swell-shrink clays and the sampling locations.

Types of Soil	Sampling site	Sampling depth D (m)	Bulk density ρ (g/cm^3)	Mass moisture content ω (%)	Liquid limit ω_L (%)	Plasticity limit ω_P (%)	Plasticity index I_P (%)	Particle composition (%)		
								0.05-2 mm	0.05-0.002 mm	<0.002 mm
Expansive soil	Nanning	0.5–1.5	1.78	35.8	75.8	28.4	47.4	21.83	20.81	57.36
	Baise	0.7–1.8	1.86	26.4	53.0	25.0	28.0	16.50	38.27	45.23
Lateritic clay	Guilin	2.0–4.0	1.85	34.9	70.3	39.8	30.5	14.30	32.20	53.50
	Liuzhou	0.5–3.0	1.78	42.4	72.6	45.9	26.7	11.71	40.83	47.59
	Laibin	2.0–3.0	1.64	41.0	82.0	46.2	35.8	12.85	40.85	46.30
	Wuming	0.5–3.0	1.70	34.3	83.0	54.1	28.9	26.80	59.55	13.65

and Baise samples were 91% and 59%, respectively, and their linear shrinkage ratios were 10.6% and 2.53%, respectively. According to the standard for swell-shrink clays (Soil Mechanics teaching group of Department of Civil Engineering in Guangxi University, 1977), all of the lateritic clays had low swell properties and were dominated by shrinkage forms. The Baise expansive soil had a low swell shrinking property, but it was dominated by expansion forms. The Nanning expansive soil had a significant swell-shrinking property, and was dominated by expansion forms.

Sample Preparation

Colloid particles are defined as the soil particles of < 0.002 mm according to most national standards (DL/T 5357-2006, 2006; GB/T 6730.67-2009, 2009; ASTM D 7928-2016, 2016). Clay minerals exist in these colloid particles. Thus, these colloid particles should be separated from the soil samples and collected together in order to analyze the mineral compositions of clays more precisely. In this study, a physicochemical method was adopted to separate and prepare the colloid particles according to Code for Chemical Analysis Tests of Rock and Soil for Hydropower and Water Conservancy Engineering (DL/T 5357-2006, 2006). The specific steps of the procedure were as follows:

(1) The soil samples were air-dried, crushed, and passed through a 0.075 mm sieve. These soil particles smaller than 0.075 mm were named as "finely ground samples (FGS)." Then, ~30–40 g of FGS was weighed, placed in a small beaker, and moistened with distilled deionized (DDI) water according to the amount of sample.

(2) ~100–200 mL of 0.1 mol/L hydrochloric acid was added to the beaker and stirred to decompose thoroughly the carbonate and other soluble salts in the soil sample. Then, the solution was allowed to settle until it became clear. The upper part of the clear liquid was decanted.

(3) The residual solution was retained and treated with dilute hydrochloric acid (pH = 4), and the upper part of clear liquid was filtered by air extraction. This operation was repeated to remove all of the calcium and magnesium ions from the solution. The ammonia buffer solution (pH = 10) plus an appropriate amount of acid chrome blue K-naphthol green B (K-B) indicator was used to test the presence of calcium and magnesium ions in the solution.

(4) After removing all of the calcium and magnesium, the sample solution was washed with DDI water and filtered by air extraction until reaching a negative chloride test with silver nitrate solution.

(5) The sample solution was placed in a 40°C constant-temperature water bath. Approximately 40 mL of 30% hydrogen peroxide was added to the sample solution. Then, the sample solution was stirred continuously to dissolve any organic matter (OM).

(6) 40 mL of sodium citrate buffer was added to the sample solution and the solution was placed in an 80°C constant-temperature water bath. Approximately 2 g of sodium hydrosulfite ($Na_2S_2O_{24}$) powder was added gradually to

Table 2 Basic swelling and shrinkage indicators of the swell-shrink clays and the sampling locations.

Types of Soil	Sampling site	Sampling depth D (m)	Free swelling ratio δ_{ef} (%)	Linear shrinkage ratio e_{sl} (%)	Volumetric shrinkage ratio e_s (%)	Shrinkage coefficient λ (%)	Shrinkage limit ω_s (%)
Expansive soil	Nanning	0.5–1.5	91	10.60	26.10	0.61	18.90
	Baise	0.7–1.8	59	2.53	6.82	0.59	14.69
Lateritic clay	Guilin	2.0–4.0	35	3.52	9.65	0.35	26.90
	Liuzhou	0.5–3.0	19	4.51	12.54	0.37	29.75
	Laibin	2.0–3.0	22	3.63	17.98	0.34	34.20
	Wuming	0.5–3.0	39	0.38	3.68	0.21	32.50

https://doi.org/10.1007/s42860-019-00056-7 Published online by Cambridge University Press

the solution under constant stirring in order to remove any iron cement from the sample.

(7) The sample solution processed with the aforementioned steps was removed to a beaker. Then, 2% sodium carbonate solution was added to the beaker to make the pH of solution ~9–10. The solution was boiled for 5 min accompanied with constant stirring. This process was called "Alkali dispersion," including removing free oxides of silicon and aluminum.

(8) The processed sample solution was placed in a 2000 mL beaker, agitated 20 times with a porous agitator, allowed to stand at constant temperature for 6 h, then the top 10 cm of supernatant was decanted using a hooked syphon and saved in a beaker. This process (Step 8) was repeated four times.

(9) The aforementioned suspension was flocculated with dilute hydrochloric acid (pH = 4). The supernatant was decanted and the flocculated <0.002 mm particles were placed in a glass dish, dried, ground with an agate mortar and pestle, labeled "Colloid particle samples (CPS)," and saved for later experiments.

Three soils (Nanning expansive soil, Baise expansive soil, and Wuming lateritic clay) were selected as representative samples to conduct the aforementioned preparation steps. In order to identify the different samples , the types and symbols of soil samples prepared for different analysis test in this study are listed in Table 3.

Analytical Methods

Differential thermal analyses (DTA). Differential thermal analyses (DTA) were performed using a Labsys simultaneous thermal analyzer (Setaram Instrumentation, Caluire, France). The experimental conditions were as follows: the temperature range was room temperature (RT) to 1000°C with a heating rate of 10°C/min and cooling rate of 50°C/min; the crucible and reference sample were pure Al_2O_3. Test samples were Nanning expansive soil, Baise expansive soil, and Wuming lateritic clay (Table 3).

XRD analyses. The XRD analyses were performed at 25°C using an X'pert PRO X-ray diffractometer (PANalytical B.V., Almelo, Netherlands), equipped with a Cu tube (λ = 0.15418 nm), over the diffraction angle range of 4–32°2θ with angular resolution of 0.0001°2θ. The scanning rate and step size were 6°2θ/min and 0.017°2θ, respectively. Test samples were Nanning expansive soil, Baise expansive soil, Wuming lateritic clay, Guilin lateritic clay, Liuzhou lateritic clay, and Laibin lateritic clay (Table 3). All of the samples were prepared using the wafer pressing method (Moore and Reynolds 1997).

XRF analyses. The XRF analyses were performed using an Axios X-ray fluorescence analyzer (PANalytical B.V., Almelo, Netherlands) equipped with a Rh-anode SST-maX operating at a power of 2.4 kW. The test samples were the same as for XRD. The experimental procedures and sample preparation of the metallic elements were based on Standards JY/T016-1996 (1996). The specimens were made using the molten sheet method (Moore and Reynolds 1997). Carbon was measured using atomic absorption spectrometry (AAS) according to the Standard GB/T 6730.67-2009 (2009). The mass percentage accuracy was 0.01%.

In order to verify the accuracy of the XRF analyses, a Chemical Element Analysis of three of the six soils mentioned above, i.e. the Baise expansive soil, the Nanning expansive soil, and the Wuming lateritic clay, was conducted at the Testing Center at the Guilin University of Technology.

Table 3 The types of and symbols used for the various soil samples.

			Soil samples Analysis test				
Soil types	Samples prepared	Sample symbols	DTA	XRD	XRF	Elemental Analysis	Zeta potential
Nanning expansive soil	Original sample	NN-O	✓	✓	✓	✓	✓
	Finely-ground sample	NN-F		✓			
	Colloid-particle sample	NN-C	✓	✓			
Baise expansive soil	Original sample	BS-O	✓	✓	✓	✓	✓
	Finely-ground sample	BS-F		✓			
	Colloid-particle sample	BS-C	✓	✓			
Wuming lateritic clay	Original sample	WM-O	✓	✓	✓	✓	✓
	Finely-ground sample	WM-F		✓			
	Colloid-particle sample	WM-C	✓	✓			
Guilin lateritic clay	Original sample	GL-O		✓	✓		✓
Liuzhou lateritic clay	Original sample	LZ-O		✓	✓		✓
Laibin lateritic clay	Original sample	LB-O		✓	✓		✓

Note: Original sample – a natural, disturbed soil powder that has not undergone chemical treatment; Finely-ground sample – soil particles of < 0.075 mm; Colloid-particle sample – flocculated particles of < 0.002 mm.

https://doi.org/10.1007/s42860-019-00056-7 Published online by Cambridge University Press

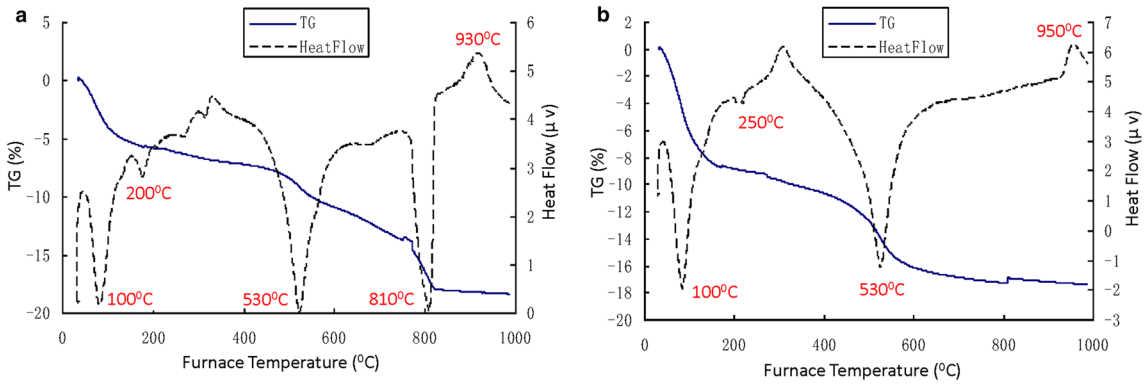

Fig. 2 DTA curves for Baise expansive soil. **a** BS-O (original sample); **b** BS-C (colloid-particle sample)

Bogue quantitative analysis method. The Bogue method, which is also known as the algebraic method, provides a means by which the mineralogical content of a soil may be calculated from XRD and elemental analyses. It obeys the following postulates (Aldridge 1982): (1) In the soil specimens, only the minerals detected by XRD are used, while minerals detected only by other methods are ignored. That is, the sum of the mineral contents observed by XRD is 100%. (2) If a mineral contains an element that no other mineral contains, that element can be used to determine the amount of that mineral in the soil specimens. Based on these two assumptions, the mineralogical composition (x, y, z) of each soil may be calculated from the ratios (a_n, b_n, c_n) between the molecular weights of the elements and the theoretical molecular weights of the minerals containing those elements, and the percentages of the various elements (A, B, C) determined by elemental analysis (Lu et al. 2012). For a system where three such elements and three mineral phases are identified, the equation is:

$$\begin{aligned} a_1x + b_1y + c_1z &= A \\ a_2x + b_2y + c_2z &= B \\ a_3x + b_3y + c_3z &= C \end{aligned} \quad (1)$$

If an element is present in only one of the minerals, Eq. 1 reduces to

$$\begin{aligned} a_1x &= A \\ b_2y &= B \\ c_3z &= C \end{aligned} \quad (2)$$

Zeta potential test. The zeta (ζ) potential was measured using a Zetasizer Nano ZS90 potentiometer (Malvern Panalytical Ltd, Malvern, United Kingdom), equipped with a microprocessor. Before and after each measurement, a type-II ultraviolet A microelectrophoresis cell was washed with DDI water to prevent cross-contamination. After each measurement, the pH of the solution was measured. If changes occurred in the pH of the solution, the last measured pH was recorded as the pH of the solution. The reliability of the zeta potential measurement was determined by using the standard deviation (SD) of the readings. The SD values were calculated from readings taken using the zeta meter (Kaya and Yukselen 2005). The SD of each measurement was <2 mV and was automatically calculated by the instrument. The zeta potentials of at least six particles for each sample were determined, and their average was taken. The room temperature was 22.5 ± 2.5°C during the experiments.

Test samples were of Nanning expansive soil, Baise expansive soil, Wuming lateritic clay, Guilin lateritic clay, Liuzhou lateritic clay, and Laibin lateritic clay (Table 3). The samples were purified by washing several times with ammonium

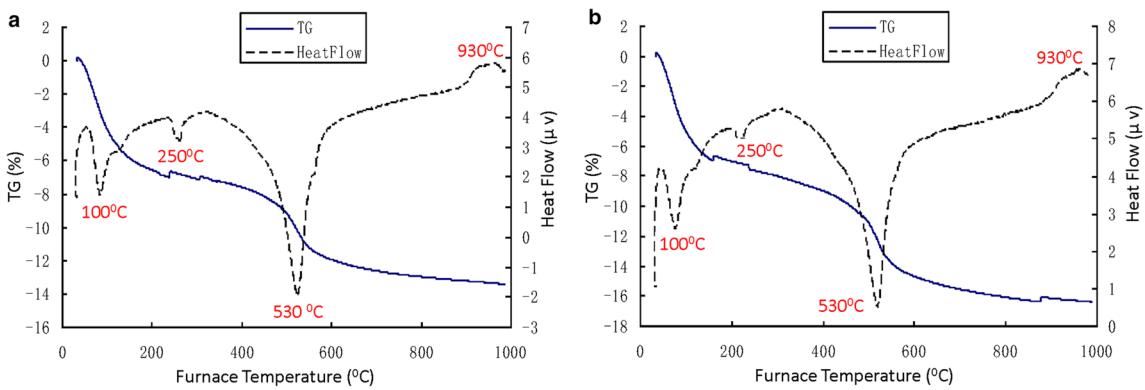

Fig. 3 DTA curves for Nanning expansive soil. **a** NN-O (original sample); **b** NN-C (colloid-particle sample)

https://doi.org/10.1007/s42860-019-00056-7 Published online by Cambridge University Press

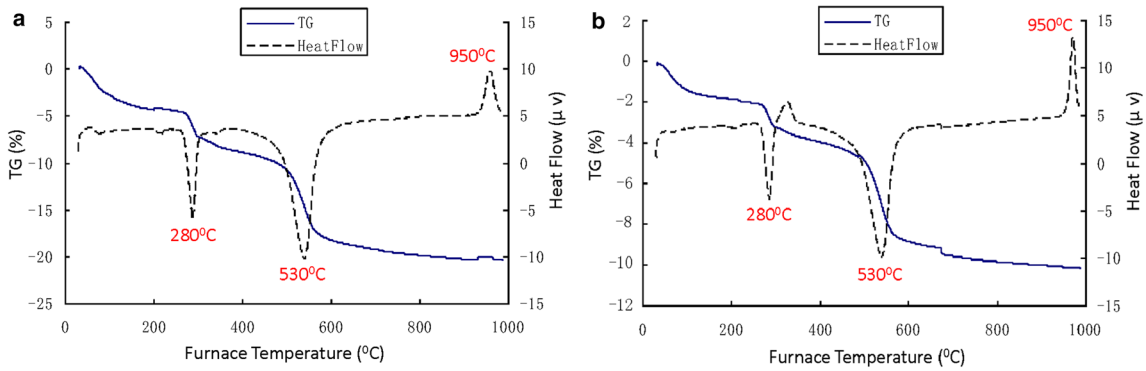

Fig. 4 DTA curves for Wuming lateritic clay. **a** WM-O (original sample); **b** WM-C (colloid-particle sample).

acetate ($CH_3CO_2NH_4$). The washing process was as follows: each as-received sample was mixed with 2 M ammonium acetate for 15 min at a solid : liquid ratio of 1:2. The supernatant was discarded when the samples had settled. The sample was considered purified when the electrical conductivity of the supernatant changed negligibly. Then, the washed sample was dried at 80°C for > 48 h and sieved through a 75 μm mesh. For the zeta potential measurements, a 50 mg sample was transferred to a 50 mL glass beaker, to which 50 mL of DDI water and a magnetic stirring bar were added. The pH of the solution (pH = 7) was measured using an Orion pH electrode (Orion Research, Massachusetts, USA).

RESULTS

Qualitative Analysis of Mineral Composition

In terms of the identification of clay minerals, DTA and XRD are mature techniques. However, the mineral compositions of the swell-shrink clays from Guangxi are so complicated that obtaining accurate and comprehensive results for these clays is difficult using a single identification method. In the present study study both DTA and XRD were used comprehensively to identify the mineral in the soil samples. By comparing and analyzing the various identification results, the mineral information for the soil samples was obtained.

DTA test results. The DTA test results (Figs 2, 3, and 4) showed that several obvious endothermic/exothermic peaks existed on each DTA curve over various temperature ranges (Table 4). The basic criteria for identifying minerals were described by Huang (1987) (Table 5).

Minerals such as Mnt and Kln were easily identified in the three clays examined (Tables 4 and 5). For example, the presence of Mnt and Kln in the expansive soils from Baise and Nanning was inferred easily from their characteristic peaks. However, Wuming lateritic clay was inferred to contain only Kln without Mnt due to the lack of an endothermic reaction peak at 100°C (Table 4). Peaks characteristic of illite (Ilt) in the expansive soils from Baise and Nanning were also observed, so the presence of Ilt was inferred in these two samples. This conclusion was also reached by Liao et al. (1984), who observed that the mineral composition of the Nanning expansive soil was dominated by Ilt. Thus, Mnt, Kln, and Ilt were present in the Nanning expansive soil. In the case of Wuming lateritic clay, a moderate endothermic reaction peak appearing at 280°C indicated the presence of gibbsite (Gbs) in this clay. Thus, Kln and Gbs were present in Wuming lateritic clay.

Compared with the colloid particle sample of the Baise sample (BS-C), a strong endothermic peak appeared at about ~800°C in the original sample (BS-O), with an intensity similar to that of the two endothermic peaks described above. One possible explanation for this was that the mineral was removed in the form of a soluble salt during the extraction process. The mineral was inferred to be calcite (Cal) (Table 5). This inference was verified by the process for the extraction of the <0.002 mm colloid particles. During this process, the Baise sample underwent a vigorous reaction when hydrochloric acid was added, which produced a large amount of carbon dioxide bubbles. Therefore, Mnt, Kln, Ilt, and Cal were present in the Baise expansive soil.

Based on the aforementioned analyses, the main minerals in each clay were initially identified. However, whether other minerals were present, such as mica-like clay minerals, quartz (Qz), etc., was difficult to judge. Thus, the possible presence of other minerals still needed to be verified using other experimental methods.

XRD results. The XRD results were processed into X-ray diffraction curves using the X 'pert *HighScore Plus* software, which was based on the Bragg equation (Moore and Reynolds 1997; Tan and Kong 2006) (Fig. 5). Several XRD peaks with various diffraction intensities appeared at various positions on the XRD curves (Fig. 5, Table 6) and possible mineral components were identified using the PDF2-2004 Card of the ICDD (International Centre for Diffraction Data). Using this information, the minerals in each swell-shrink soil were identified easily. For example, the Baise expansive soil revealed three distinct diffraction peaks, at 4.5, 4.25, and 3.33 Å, in all of the particle-size fractions (Fig. 5a). The reflections at 4.25 Å and 3.33 Å peaks are characteristic of Qz (Table 6); with that at 3.33 Å being the most intense and, thus, given the rank of 100. In addition, the intensity of the 4.5 Å peak is usually recognized as the combined intensity of clay minerals (Moore and Reynolds 1997). Therefore, some Qz particles were present in the Baise expansive soil. Furthermore, the 3.0 Å peak appeared in both the original and

https://doi.org/10.1007/s42860-019-00056-7 Published online by Cambridge University Press

Table 4 Endothermic/exothermic peaks of swell-shrink clays at various temperatures on the DTA curves.

Soil specimen		Temperature range of endothermic/exothermic peak				
		100°C	200–400°C	500–550°C	800°C	900–1000°C
Baise expansive soil	Original sample	100°C-Endothermic (S)	200°C-Endothermic (W)	530°C-Endothermic (S)	810°C - Endothermic (S)	930°C-Exothermic (W)
	Colloid-particle sample	100°C-Endothermic (S)	250°C-Endothermic (W)	530°C-Endothermic (S)	×	950°C-Exothermic (W)
Nanning expansive soil	Original sample	100°C-Endothermic (M)	250°C-Endothermic (W)	530°C-Endothermic (S)	×	930°C-Exothermic (W)
	Colloid-particle sample	100°C-Endothermic (M)	250°C-Endothermic (W)	530°C-Endothermic (S)	×	930°C-Exothermic (W)
Wuming lateritic clay	Original sample	×	280°C-Endothermic (M)	530°C-Endothermic (S)	×	950°C-Exothermic (M)
	Colloid-particle sample	×	280°C-Endothermic (M)	530°C-Endothermic (S)	×	950°C-Exothermic (M)

Notes: ×—No endothermic/exothermic peak; T°C -Endothermic (S) – A strong endothermic peak at T°C; T°C -Exothermic (W) – A weak exothermic peak at T°C; T – Temperature value; S – Strong; M – Moderate; W – Weak.

Table 5 The basic criteria used to identify minerals.

Mineral	Descriptions of the characteristic peak
Montmorillonite	A strong endothermic reaction peak appears at ~100°C due to the removal of adsorbed water, and a weak exothermic reaction peak appears at 900–1000°C due to the decomposition of aluminum monoxide and mullite during the montmorillonite reaction.
Kaolinite	A strong endothermic reaction occurs at 500–550°C, producing broad and sharp endothermic peaks.
Illite	A weak endothermic reaction peak appears below 250°C due primarily to the discharge of adsorbed water. This phenomenon is similar to the peak formed by Mnt, but the intensity of the endothermic peak is much weaker than that of the Mnt peak. At ~550°C, Ilt undergoes a dehydroxylation process in which its structural water is discharged. Then, a weak endothermic reaction occurs at 850–1000°C when the residual structural water is discharged and the structure is completely destroyed. Immediately after this, a weak exothermic peak appears at 1000°C when the crystals break down to form mullite and spinel.
Calcite	A strong endothermic reaction occurs at ~800°C producing a strong endothermic peak.
Gibbsite	A strong endothermic reaction peak appears at 200–400°C due to the drainage of structural water and the formation of soft bauxite.

the FGS samples, but was not present in the CPS sample. This indicated that the mineral represented by this peak was a soluble salt. Cal produces a strong diffraction peak at 3.0 Å, and dissolves in strong acids. Thus, Cal probably dissolved in the hydrochloric acid solution used during the preparation of the CPS sample. This phenomenon occurred during the sample-preparation process and was verified by the DTA test result. Therefore, a certain amount of Cal must be present in the Baise expansive soil. By comparing the diffraction patterns of the original and FGS samples (Fig. 5a), identical diffraction peaks were present in both at the same position with similar peak intensities, indicating that the <0.075 mm mineral particles dominate the Baise expansive soil.

In the CPS sample, in addition to the XRD peaks described above, other distinct diffraction peaks appeared at 15, 10, 7.2, 4.98, and 3.56 Å. The peak at 15 Å is characteristic of Mnt; the 10 and 5 Å peaks are characteristic of Ilt, and the 7.2 and 3.56 Å peaks were characteristic of Kln. Thus, Mnt, Ilt, and Kln were all present in the Baise sample. However, whether Mnt was in its Ca- or Na-exchanged form was not differentiated.

DTA analysis determined that the Baise sample contains Qz, Mnt, Kln, and Cal. The presence of the last three minerals was also confirmed by the XRD analyses.

The same analyses were conducted on other clays. The Wuming CPS sample lacked the 4.17 Å peak that was present in both the original and FGS samples. This peak is characteristic of goethite (Gth), so some Gth was inferred to be present in the Wuming lateritic clay, but not in its colloidal fraction. This conclusion was supported by the color variations of the samples. The iron in Gth is red. The colors of the original sample and the FGS

https://doi.org/10.1007/s42860-019-00056-7 Published online by Cambridge University Press

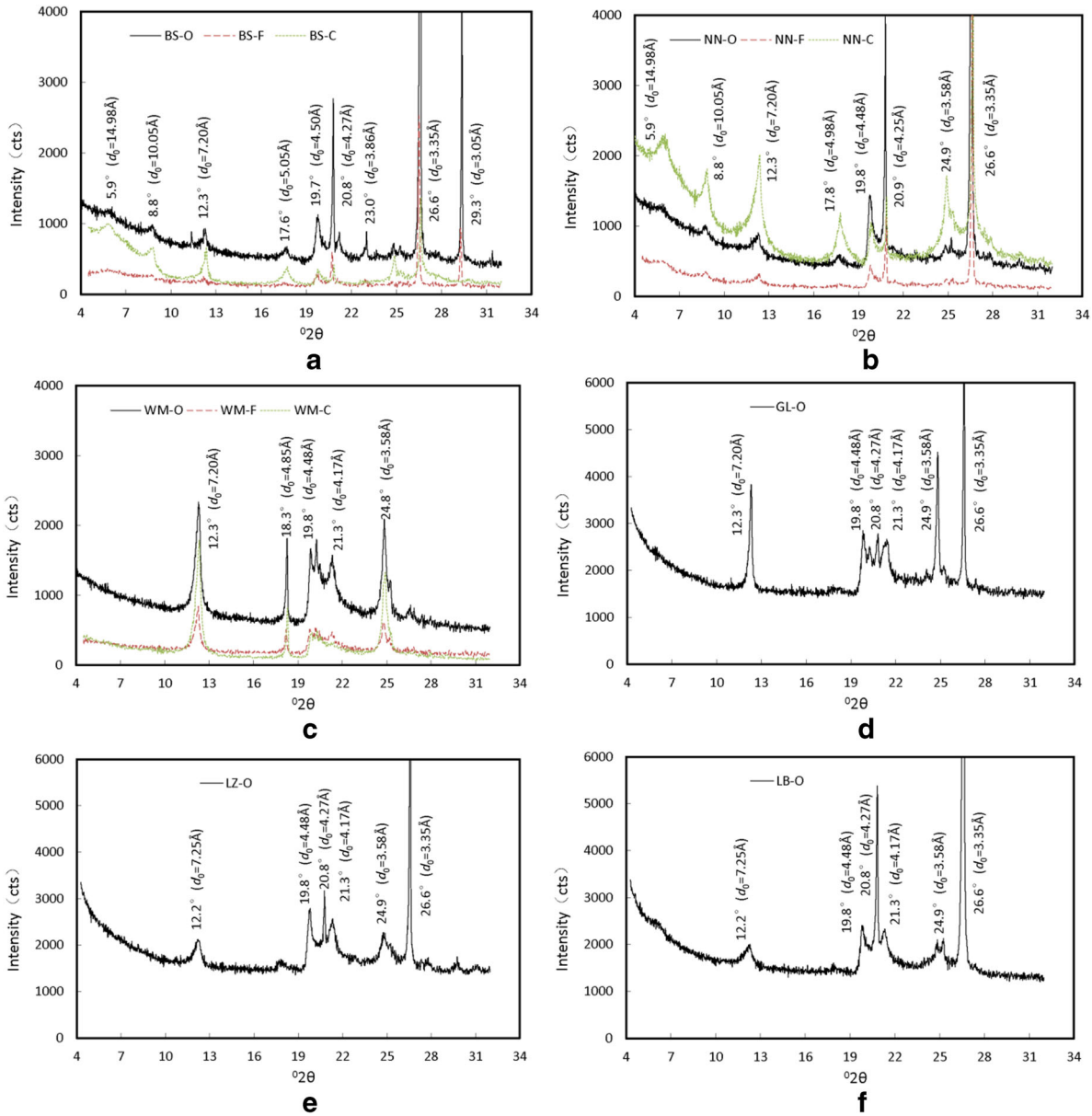

Fig. 5 XRD curves of six tested soils. **a** Baise expansive soil; **b** Nanning expansive soil; **c** Wuming lateritic clay; **d** Guilin lateritic clay; **e** Liuzhou lateritic clay; **f** Laibin lateritic clay.

were red, but the colloidal fraction was white, thus demonstrating that Gth was eliminated by the Na hydrosulfite treatment.

In summary, DTA and XRD results indicated that the Baise and Nanning expansive soils were composed mainly of Qz, Mnt, Ilt, and Kln, and the Baise soil also contained Cal. The lateritic clays from Guilin, Liuzhou, and Laibin contained mainly Kln, Gth, and Qz, while the Wuming sample contained mainly Kln, Gth, and Gbs.

Quantitative Analysis of Mineral Composition

Mineral type and mineral content are the main factors influencing the physical-mechanical and engineering properties of swell-shrink soils (Mitchell and Soga 2005). These differentiations can be difficult due to the complexity of the soils, but an attempt was made to make a rough quantitative analysis of the mineral composition of six soils using XRF analysis and the Bogue method.

XRF analyses. The accuracy of the XRF analysis results from these six soils (Table 7) was determined by submitting three of them, namely Baise, Nanning, and Wuming, to further chemical elemental analysis, conducted at the Testing Center at the Guilin University of Technology (Table 8). Comparing the test results of each element from XRF (Table 7) and chemical analysis (Table 8) revealed that the major element compositions were almost identical. The small differences (–2.74% to 0.74%), which were within the error range, resulted primarily from the inhomogeneity of soil

https://doi.org/10.1007/s42860-019-00056-7 Published online by Cambridge University Press

Table 6 The position and relative intensity of the XRD peaks of standard clay minerals and swell-shrink clays on the XRD curves.

Soil specimen		The position and relative strength of the XRD peaks										
Standard clay mineral		Quartz		Combined clay mineral	Calcite	Montmorillonite	Illite		Kaolinite		Gibbsite	Goethite
		3.33 Å	4.25 Å	4.5 Å	3.0 Å	15.0 Å	5.0 Å	10.0 Å	3.56 Å	7.2 Å	4.8 Å	4.17 Å
Baise expansive soil	Original sample	3.35 Å (H)	4.27 Å (M)	4.50 Å (M)	3.05 Å (M)	14.98 Å (L)	5.05 Å (L)	10.05 Å (L)	3.86 Å (L)	7.20 Å (L)	×	×
	Finely-ground sample	3.36 Å (H)	4.29 Å (M)	4.50 Å (M)	3.05 Å (M)	14.95 Å (L)	5.05 Å (L)	10.05 Å (L)	3.88 Å (L)	7.20 Å (L)	×	×
	Colloid-particle sample	3.35 Å (H)	4.26 Å (M)	4.48 Å (M)	×	14.94 Å (M)	5.05 Å (M)	10.05 Å (M)	3.58 Å (M)	7.20 Å (M)	×	×
Nanning expansive soil	Original sample	3.35 Å (H)	4.26 Å (M)	4.50 Å (M)	×	15.05 Å (L)	5.02 Å (L)	10.05 Å (L)	×	7.18 Å (L)	×	×
	Finely-ground sample	3.35 Å (H)	4.26 Å (M)	4.48 Å (M)	×	14.87 Å (L)	5.00 Å (L)	10.05 Å (L)	×	7.18 Å (L)	×	×
	Colloid-particle sample	3.35 Å (H)	4.25 Å (M)	4.48 Å (M)	×	14.98 Å (M)	4.98 Å (M)	10.05 Å (M)	3.58 Å (M)	7.20 Å (M)	×	×
Wuming lateritic clay	Original sample	×	×	4.48 Å (M)	×	×	×	×	3.58 Å (H)	7.20 Å (H)	4.85 Å (H)	4.17 Å (M)
	Finely-ground sample	×	×	4.48 Å (M)	×	×	×	×	3.59 Å (H)	7.20 Å (H)	4.87 Å (H)	4.18 Å (M)
	Colloid-particle sample	×	×	4.46 Å (M)	×	×	×	×	3.58 Å (H)	7.20 Å (H)	4.85 Å (H)	×
Guilin lateritic clay (Original)		3.35 Å (H)	4.27 Å (M)	4.47 Å (M)	×	×	×	×	3.58 Å (H)	7.20 Å (H)	×	4.16 Å (M)
Liuzhou lateritic clay (Original)		3.35 Å (H)	4.27 Å (M)	4.48 Å (M)	×	×	×	×	3.58 Å (M)	7.25 Å (M)	×	4.17 Å (M)
Laibin lateritic clay (Original)		3.35 Å (H)	4.27 Å (M)	4.48 Å (M)	×	×	×	×	3.58 Å (L)	7.25 Å (L)	×	4.17 Å (M)

Note: × – No diffraction peak; (H) – High relative intensity; (M) – Moderate relative intensity; (L) – Low relative intensity.

Table 7 Results of element analysis by X-ray fluorescence.

Soil type	Major element composition (wt.%)							SiO_2/Al_2O_3
	SiO_2	Al_2O_3	Fe_2O_3	K_2O	Na_2O	MgO	C	
Baise expansive soil	53.18	16.27	ND	1.89	0.16	0.91	1.72	3.27
Nanning expansive soil	64.31	22.58	ND	2.22	0.22	0.81	ND	2.85
Wuming lateritic clay	36.48	37.32	8.53	ND	ND	ND	ND	0.98
Guilin lateritic clay	41.96	28.12	14.85	ND	ND	ND	ND	1.49
Liuzhou lateritic clay	42.60	27.91	12.85	ND	ND	ND	ND	1.53
Laibin lateritic clay	58.61	18.50	10.64	ND	ND	ND	ND	3.17

Note: ND = not detected.

specimens. Therefore, the XRF results for the six soils in reality reflected the actual mineral contents of these soils.

Bogue method of quantitative analysis of mineral composition. The Bogue method (Lu et al. 2012) was used to calculate the mineral compositions of the six test soils. Calculations for the Baise expansive soil are described below and are representative of the calculations used for all six of the samples.

(1) XRD results revealed that the Baise expansive soil contained Qz, Kln, Ilt, Mnt, and Cal (Table 6), but the elements Ca, Na, and K appeared only in Cal, Mnt, and Ilt (Table 9), respectively, so Eq. 2 can be applied to calculate the respective proportions, P_i, of each of these minerals in the Baise sample, using data from Tables 7 and 9:

$$\begin{aligned} a_1x &= \frac{12}{100}P_{Cal} = 1.72 \\ b_2y &= \frac{38{\cdot}0.3}{363.3{\cdot}2}P_{Mnt} = 0.16 \\ c_3z &= \frac{94{\cdot}0.5}{406.5{\cdot}2}P_{Ilt} = 1.89 \end{aligned} \quad (3)$$

Then, solving for P_i gives

$$\begin{aligned} P_{Cal} &= 1.72{\cdot}\frac{100}{12} = 14.33\% \\ P_{Mnt} &= 0.16{\cdot}\frac{363.3{\cdot}2}{38{\cdot}0.3} = 10.20\% \\ P_{Ilt} &= 1.89{\cdot}\frac{406.5{\cdot}2}{94{\cdot}0.5} = 32.69\% \end{aligned} \quad (4)$$

However, the Baise sample contains not only Cal, Ilt, and Mnt, the proportions of which are now already known from Eq. 4, but it also contains Kln. The proportion of Kln ($x = P_{Kln}$) can be calculated from Eq. 5 after recognizing that Kln, Ilt, and Mnt all contain aluminum (given by the variable A):

$$a_1x + b_1y + c_1z = A \quad (5)$$

Or

$$a_1P_{Kln} + b_1P_{Ilt} + c_1P_{Mnt} = Al \quad (6)$$

Solving for P_{Kln} and substituting values for a_1, b_1, c_1, P_{Ilt}, and P_{Mnt} gives

$$\begin{aligned} P_{Kln} &= \frac{Al - b_1P_{Ilt} - c_1P_{Mnt}}{a_1} \\ &= \frac{16.27 - \frac{102}{406.5}\frac{2}{3}32.69 - \frac{102}{363.3}10.20}{\frac{102}{258}} = 2.79\% \end{aligned} \quad (7)$$

Similarly, Qz, Kln, Ilt, and Mnt all contain silicon. The Ilt, Mnt, and Kln contents are now known, so the Qz content can be calculated in the same manner, giving $P_{Qz} = 25.84\%$.

The accuracy of the Bogue method is easily calculated as the difference between 100% and the sum of fractions of the respective minerals identified by XRD, i.e.

Table 8 Analytical results of element analyses.

Soil type	Major element composition (%)							SiO_2/Al_2O_3
	SiO_2	Al_2O_3	Fe_2O_3	K_2O	Na_2O	CaO	MgO	
Baise expansive soil	53.63	17.01	5.74	2.21	0.21	5.71	1.15	3.15
Nanning expansive soil	63.19	20.34	2.45	2.50	0.23	0.21	1.01	3.10
Wuming lateritic clay	36.27	37.71	8.66	0.31	0.07	0.13	0.12	0.96

https://doi.org/10.1007/s42860-019-00056-7 Published online by Cambridge University Press

Table 9 Theoretical molecular weights and amounts present of the minerals and elements in Baise expansive soil.

Material types		Theoretical molecular formula	Theoretical molecular weight	Content (%)
Minerals	Quartz	SiO_2	60	Unknown P_{quartz}
	Kaolinite	$Al_2Si_2O_5(OH)_4$	258	Unknown $P_{kaolinite}$
	Illite	$Al_3H_2K_{0.5}O_{12}Si_4$	406.5	Unknown P_{illite}
	Montmorillonite	$Na_{0.3}Al_2Si_4O_{12}H_2{\cdot}nH_2O$	363.3	Unknown $P_{montmorillonite}$
	Calcite	$CaCO_3$	100	Unknown $P_{calcite}$
Elements	Silicon dioxide	SiO_2	60	53.18
	Aluminum oxide	Al_2O_3	102	16.27
	Potassium oxide	K_2O	94	1.89
	Sodium oxide	Na_2O	38	0.16
	Carbon	C	12	1.72

$$Deviation(\%) = 100 - \sum_i P_i$$

For the Baise soil, the error is, therefore:

$$Deviation = 100 - (14.33 + 10.20 + 32.69 + 2.79 + 25.84) = 14.15\%$$

The Nanning expansive soil was calculated in the same way (Table 10), as were the mineral compositions of the lateritic soils (Table 10), except data for the latter were also obtained from Table 11.

The deviation from 100% of the calculated mineralogical compositions of the expansive soils (i.e. 14.15% for the Baise specimen and 9.53% for the Nanning specimen) were relatively large due to their complex mineral compositions. The essential reason was that the Bogue method has its limits. When the numbers of mineral types in the soil are more than the numbers of calculation equations, the Bogue method should be used with other methods such as the K-value method (Lu et al. 2012). However, the total mineral deviations of the lateritic clays were relatively small and ranged from 2.43 to 5.34%. The reason was that the lateritic clays contained fewer main minerals and the mineral types were relatively uniform. In summary, these deviations are within the acceptable range, which indicated that the Bogue method can be applied satisfactorily to these swell-shrink soils.

Kln was a dominant mineral in the lateritic clays (Table 10). The Kln contents of the Wuming, Guilin, and Liuzhou samples ranged from 70 to 80%, while in the Laibin lateritic clay the value was ~50%. These results were consistent with the conclusions of previous studies (Sun et al. 2014; Ye 2017; Zhu et al. 2019). All of the lateritic clays contained ~10% Gth, which suggested that the lateritic clays were rich in iron minerals. In other words, the typical lateritic clays were composed primarily of iron-rich minerals. This is also the principal reason why lateritic clays are often red and brown in color. In the expansive soils from Baise and Nanning, Ilt was the most abundant mineral, ranging from 30 to 40% (Tan and Kong 2006). Qz was the second most abundant mineral, ranging from 25 to 30%. The Mnt content of the Nanning sample was larger than that of the Baise sample, resulting in differences in their expansive characteristics (Table 2).

Zeta Potential Analysis

The zeta potentials of all of the clay samples were negative (Table 12). The zeta potentials of the lateritic clays were relatively small, but those of the expansive soils were relatively large, which follows the expected variations in specific surface area and permanent negative layer charge, i.e. Mnt > Ilt > Kln; thus, the more Mnt the greater the surface area and layer charge in the soil.

Table 10 Summary of the mineral compositions in the soils (all values %).

Soil types	Mineral compositions and deviation from 100%							
	Quartz	Kaolinite	Illite	Montmorillonite	Gibbsite	Goethite	Calcite	Deviation (%)
Baise expansive soil	25.84	2.79	32.69	10.20	-	-	14.33	14.15
Nanning expansive soil	27.45	10.60	38.40	14.02	-	-	-	9.53
Wuming lateritic clay	-	78.43	-	-	9.65	9.49	-	2.43
Guilin lateritic clay	8.88	71.13	-	-	-	16.52	-	3.47
Liuzhou lateritic clay	14.30	70.60	-	-	-	9.76	-	5.34
Laibin lateritic clay	46.79	36.85	-	-	-	11.84	-	4.52

https://doi.org/10.1007/s42860-019-00056-7 Published online by Cambridge University Press

Table 11 Theoretical molecular weights and amounts present of the minerals and elements in Wuming lateritic clay.

Material types		Theoretical molecular formula	Theoretical molecular weight	Content (%)
Minerals	Kaolinite	$Al_2Si_2O_5(OH)_4$	258	Unknown $P_{kaolinite}$
	Gibbsite	Al(OH)3	78	Unknown $P_{gibbsite}$
	Goethite	FeO(OH)	89	Unknown $P_{goethite}$
Elements	Silicon dioxide	SiO_2	60	36.48
	Aluminum oxide	Al_2O_3	102	37.32
	Iron oxide	Fe_2O_3	160	8.53

DISCUSSION

According to clay-mineral theory (Mitchell and Soga 2005), mineral composition is not only the sole index of the dielectric condition of swell-shrink clays, but it is also a determinant of the clay's physical-mechanical properties, especially the expansion and contraction characteristics. The electrical double layer (DL) is an important factor for explaining the aforementioned properties of soils. Zeta potential, which reflects the properties of the DL, is a critical parameter for this explanation process. Therefore, a discussion of the relationships between the zeta potential and swelling indexes with respect to of mineral compositions in soils is necessary.

The dominant minerals in the Baise and Nanning expansive soils were Mnt and Ilt (Table 10) so both had large specific surface areas and a high degree of isomorphous substitution, resulting in more negative charge (Table 12). The Nanning expansive soil had greater Mnt and Ilt contents than the Baise expansive soil, so the Nanning expansive soil had a greater zeta potential than the Baise expansive soil. However, the lateritic clays from Wuming, Guilin, Liuzhou, and Laibin, the main mineral of which was Kln, had relatively weak or no crystal replacement, resulting in less negative charge (Table 12). In addition, the lateritic clays had ~10% Gth, which easily generated protonation of the hydroxyl ion on the surface of iron oxide, resulting in a positive charge on the surface of the particles. This positive charge can inhibit the generation of negative charge. Therefore, compared with expansive soils, the zeta potentials of the lateritic clays were much smaller. The result was verified easily by the measurement of specific surface area of these six clays. The Nanning expansive soil had the largest specific surface area (112.35 m^2/g) while the Liuzhou lateritic clay had the smallest (43.08 m^2/g) .

The analysis above indicates that when the free solution was neutral water (i.e. pH=7), the magnitude and signal (positive and negative value) of the zeta electric potential should be related primarily to the type of minerals in the soil sample and the mineral content of the soils.

Soil mechanical theory says that the swelling characteristic is the fundamental property for swell-shrink clays. Generally, the free swelling ratio (δ_{ef}), recognized as the simplest index reflecting the swelling characteristic of a soil, is also related closely to the mineral compositions of soils. Therefore, the relationships of the δ_{ef} and zeta potential are discussed in the following text.

The relationship between the zeta potential and the free swelling ratio (δ_{ef}) (Table 2 and 12) was analyzed (Fig. 6). As shown in Fig. 6a, the free swelling ratio was related linearly to the zeta potential with a relatively high linear fitting value of 0.97 for all of the swell-shrink clays. The free swelling ratio decreased as the zeta potential decreased. However, the correlation between the free swelling ratios and the zeta potentials of the lateritic clays was not obvious (Fig. 6b). The linear fitting value was only 0.62, which was very low compared to that in Fig. 6a. The reason for these distinctions can be analyzed based on the mineral compositions of these clays determined above.

According to clay-mineral theory (Mitchell and Soga 2005), the amount of surface charge and expansion ability of clay minerals increase successively in the following order: Kln to Ilt to Mnt. Kln has the smallest surface charge, resulting in the weakest expansion ability. Mnt has the largest surface charge, resulting in the greatest expansion ability. The aforementioned mineral analysis has indicated that lateritic clays were composed primarily of Kln and Gth. Gth transforms easily into free iron oxide, which causes cementation (Wang 1983; Kong et al. 1995). Therefore, two reasons for the low fitting values of the lateritic clays were concluded as a means of comparisonn with their mineral compositions. Firstly, not all of the Kln exists entirely in a loose state of clay; some was encased in free iron oxide, forming large pellet agglomerations, which had an insignificant effect on the expansion of the lateritic clays. Secondly, as Kln was the main mineral in lateritic clays, the surfaces of the clay particles had a lower negative charge and lower water adsorption capacity. Therefore, the expansion ability of the lateritic clays was also weak.

Table 12 The zeta potential of the various clays.

Specimen type	Lateritic clays				Expansive soils	
	Laibin	Liuzhou	Guilin	Wuming	Baise	Nanning
Zeta potential (mV) (pH=7)	–4.46	–2.64	–4.59	–12.3	–21.9	–40.5

https://doi.org/10.1007/s42860-019-00056-7 Published online by Cambridge University Press

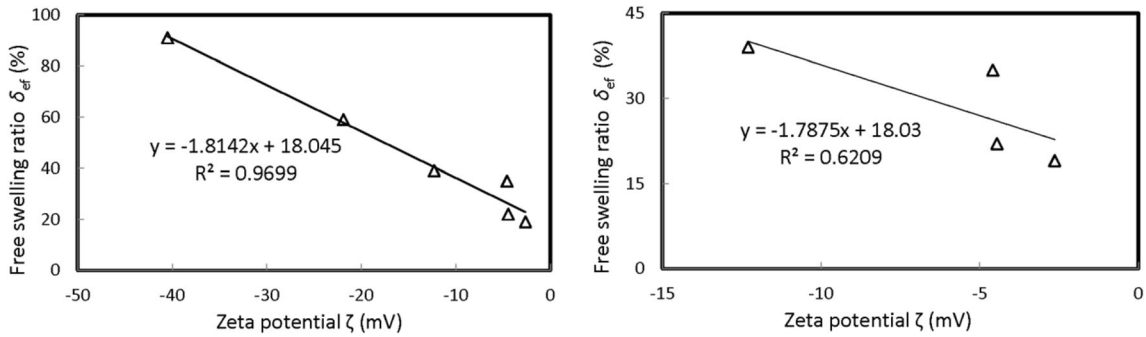

Fig. 6 Curves depicting the relationship between the free-swelling ratio and the zeta potential. **a** Swell-shrink clays; **b** lateritic clays.

These two factors resulted in a weak correlation between the free swelling ratio and the zeta potential.

In the expansive soils, the clay minerals were primarily present as dispersed clay particles, and almost all of the measured clay minerals had an impact on the swelling properties of the soil samples. As almost no cementation was present in the expansive soils, the correlation between the clay minerals and the expansion property was strong. Therefore, the effect of the zeta potential on the expansion property was strong. A strong correlation was found between the free swelling ratio and the zeta potential.

As can be seen from the analysis above, the correlation between the zeta potential and the free swelling ratio of the lateritic clays was weak and their fitting value was low. However, the addition of the expansive soils increased the correlation between the zeta potential and the free swelling ratio of all of the swell-shrink clays, so the fitting value increased significantly. This indicated that the value of the zeta potential can reflect accurately the expansion of the expansive soils. In the lateritic clays, the expansibility was affected by many factors and it was correlated weakly with the zeta potential.

In the Nanning expansive soil, Mnt was the dominant mineral, the zeta potential was greatest, the expansibility was the strongest, and the free swelling ratio was as much as 91%. In the lateritic clays, Kln was the most abundant mineral and the swelling was less. This showed that the swelling property of the swell-shrink soils was related mainly to the type of clay minerals and the mineral contents.

CONCLUSIONS

(1) Qualitative methods of analysis, such as DTA and XRD, were conducted to identify accurately the mineral compositions of the soils. The results indicated that the Baise and Nanning expansive soils are composed mainly of Qz, Mnt, Ilt, and Kln. In addition, the Baise samples also contain Cal. The lateritic clays from Guilin, Liuzhou, and Laibin contain mainly Kln, Gth, and Qz, while the Wuming sample contains mainly Kln, Gth, and Gbs.

(2) The major element compositions of the swell-shrink clays were determined by using XRF. Based on the results, the mineral composition was further analyzed quantitatively using the Bogue method. The results indicated that Kln was the dominant mineral in the lateritic clays. The Wuming, Guilin, and Liuzhou samples were 70–80% Kln, while the Laibin lateritic clay was 50% Kln. The lateritic clays contained ~10% Gth. The Baise and Nanning expansive soils contained the largest percentage of Ilt (~30–40%). Qz was the second most common mineral (~25–30%). The percentage of Mnt ranged from 10 to 15%.

(3) The relationship between the mineral compositions, zeta potentials, and free swelling ratios were briefly investigated. This investigation revealed that the zeta potential was related mainly to the type and amount of clay minerals in the soils when neutral water was used as the free solution (pH=7). The correlation between the swelling index and the zeta potential was greater for the expansive soils than for the lateritic clays, which indicated that the swelling properties of the expansive soils were more affected by the clay mineral composition than were those of the lateritic clays.

ACKNOWLEDGMENTS

The authors are grateful for the financial support provided by the National Natural Science Foundation of China [Grant No. 41962014, 51568014], the Natural Science Foundation of Guangxi Province, China [Grant No. 2018GXNSFAA138182, 2018GXNSFDA281038], the project of Guangxi Key Laboratory of New Energy and Building Energy Saving [Grant No. 17-J-21-2], and the Scientific Research Foundation for Doctor of Guilin University of Technology [Grant No. 2016254]. The authors are grateful to the editor and anonymous reviewers for their valuable comments and suggestions.

Compliance with Ethical Statements

Conflict of Interest

The authors declare that they have no conflict of interest.

Ethical Approval

This article does not contain any studies with human participants or animals performed by any of the authors.

REFERENCES

Aldridge, L. P. (1982). Accuracy and precision of phase analysis in Portland cement by Bogue, microscopic and X-ray diffraction methods. *Cement and Concrete Research, 12*, 381–398.

https://doi.org/10.1007/s42860-019-00056-7 Published online by Cambridge University Press

Arca, M. N., & Weed, S. B. (1966). Soil aggregation and porosity in relation to contents of free iron oxide and clay. *Soil Science, 101*, 164–170.

ASTM D 7928-2016 (2016). Standard Test Method for Particle-Size Distribution (Gradation) of Fine-Grained Soils Using the Sedimentation (Hydrometer) Analysis. US-ASTM.

Chorom, M., & Rengasamy, P. (1995). Dispersion and zeta potential of pure clays as related to net particle charge under varying pH, electrolyte concentration and cation type. *European Journal of Soil Science, 46*, 657–665.

Dai, S. B., Huang, J., & Xia, L. (2005). Analysis of mineral composition and chemical components of expansive soil in North Hubei. *Rock and Mechanics, 26*, 300–303.

Derjaguin, B.V. & Landau L. (1941). Theory of the stability of strongly charged lyophobic sols and of the adhesion of strongly charged particles in solutions of electrolytes. *Acta Physico-Chimica* URSS, *14*, 633.

DL/T 5357-2006 (2006). Code for Chemical Analysis Test of Rock and Soil for Hydropower and Water Conservancy Engineering. National Development and Reform Commission (NDRC) of the People's Republic of China, Beijing.

Erzin, Y., & Yukselen, Y. (2009). The use of neural networks for the prediction of zeta potential of Kln. *Mathematical Geosciences, 41*, 779–797.

Farahani, E., Emami, H., Fotovat, A., & Khorassani, R. (2019). Effect of different K:Na ratios in soil on dispersive charge, cation exchange and zeta potential. *European Journal of Soil Science, 70*, 311–320.

Feng, Y. Y., Zhang, Y. S., Qu, Y. X., & Huang, C. B. (2001). Mechanism of embankment defects caused by expansive soils in Baise Basin, Nankun railway. *Chinese Journal of Geotechnical Engineering, 23*, 463–467.

GB/T 6730.67-2009. (2009). *Iron Ores-Determination of Arsenic Content-Hydride Generation Atomic Absorption Spectrometric Method*. Beijing: China National Standardization Management Committee.

Huang, B. L. (1987). *Mineral Identification Manual of Differential Thermal Analysis*. Beijing: Science Press.

JY/T 016-1996. (1996). *General Rules for Wavelength Dispersive X-ray Fluorescence Spectrometry*. Beijing: National education committee of the People's Republic of China.

Kaya, A., & Yukselen, Y. (2005). Zeta potential of clay minerals and quartz contaminated by heavy metals. *Canadian Geotechnical Journal, 42*, 1280–1289.

Kong, L. W., Luo, H. X., & Yuan, J. X. (1995). Preliminary study on the effective cementation characteristics of the red clay. *Chinese Journal of Geotechnical Engineering, 17*, 42–47.

Li, S. L., Shi, B., & Du, Y. J. (1997). Study on the engineering geology of expansive soil in China. *Ziran Zazhi, 19*, 82–86.

Liao, S. W. (1984). *Expansive Soil and Railway Engineering*. Beijing: China Railway Press.

Lu, H. B., Zeng, Z. T., Yin, G. Q., & Zhao, Y. L. (2012). Analysis of mineral composition of red clay in Guangxi. *Journal of Engineering Geology, 20*, 651–656.

Lu, H. B., Zeng, Z. T., Ge, R. D., & Zhao, Y. L. (2013a). Experimental study of tensile strength of swell-shrink soils. *Rock and Soil Mechanics, 34*, 615–620.

Lu, H. B., Zeng, Z. T., Zhao, Y. L., Ge, R. D., Chen, C. Y., & Wei, C. F. (2013b). Function fitting on strength attenuation curve of swell-shrinking soils. *Chinese Journal of Geotechnical Engineering, 35*, 157–162.

Luo, H. X. (1983). The effect of amorphous materials on the mechanical property and structure of soil. *Rock and Mechanics, 4*, 69–74.

Madu, R. M. (1977). An investigation into the geotechnical and engineering properties of some laterites of Eastern Nigeria. *Engineering Geology, 11*, 101–125.

Marchuk, A., & Rengasamy, P. (2011). Clay behavior in suspension is related to the iconicity of clay-cation bonds. *Applied Clay Science, 53*, 754–759.

Mitchell, J. K., & Soga, K. (2005). *Fundamentals of Soil Behavior* (3rd ed.). Hoboken, New Jersey, USA: John Wiley & Sons.

Moore, D. M., & Reynolds, R. C. (1997). *X-Ray Diffraction and the Identification and Analysis of Clay Minerals* (2nd ed.). New York: Oxford University Press.

Norrish, K. (1954). Crystalline swelling of montmorillonite: Manner of swelling of montmorillonite. *Nature, 173*, 256–257.

Norrish, K., & Rausell-Colom, J. A. (1961). Low-angle X-ray diffraction studies of the swelling of montmorillonite and vermiculite. *Clays and Clay Minerals, 10*, 123–149.

Ofir, E., Oren, Y., & Adin, A. (2007). Elecro-flocculation: the effect of zeta potential on particle size. *Desalination, 204*, 33–38.

Qu, Y. X., Zhang, Y. S., Feng, Y. Y., & Zhang, J. G. (2002). Quantitative study on the clay mineral composition of expansive soils in China. *Journal of Engineering Geology, 10*, 416–422.

Shao, W. M., Tan, L. R., Zhang, M. Y., & Hua, L. L. (1994). The relation between mineral composition and swelling character of swelling soil. *Rock and Mechanics, 15*, 11–19.

SL 237-1999 (1999). Specification of Soil Test. Ministry of Water Resources of the People's Republic of China, Beijing.

Soil Mechanics teaching group of Department of Civil Engineering in Guangxi University (1977). A preliminary study on the evaluation index of expansion and contraction. *Journal of Guangxi University (Natural Science Edition)*, *1*, 21–38.

Sparks, D. L. (1986). *Soil Physical Chemistry*. Boca Raton, Florida, USA: CRC Press.

Sun, D. A., Liu, W. J., & Lu, H. B. (2014). Soil-water characteristic curve of Guilin lateritic clay. *Rock and Soil Mechanics, 35*, 3345–3351.

Sun, D. A., Gao, Y., Zhou, A. N., & Sheng, D. C. (2016). Soil-water retention curves and microstructures of undisturbed and compacted Guilin lateritic clay. *Bulletin of Engineering Geology and the Environment, 75*, 781–791.

Tan, L. R. (1984). Quantitative analysis of clay minerals - A method study. *Acta Mineralogical Sinica, 4*, 71–77.

Tan, L. R. (1997). Study on mechanism of expansion and shrinkage of the montmorillonite crystal. *Rock and Mechanics, 18*, 13–18.

Tan, L. R., & Kong, L. W. (2001). Study on the swelling and shrinkage of montmorillonite crystal and its relationship with matrix suction. *Science in China (Series D), 31*, 119–126.

Tan, L. R., & Kong, L. W. (2006). *Special Geotechnical Engineering Soil Science*. Beijing: Science Press.

Van Olphen, H. (1977). *An Introduction to Clay Colloid Chemistry*. New York: Wiley chapter 7.

Verwey, E. J. W., & Overbeek, J. T. G. (1948). *Theory of the Stability of Lyophobic Colloid*. Amsterdam: Elsevier.

Wang, J. Z. (1983). The effects of free iron oxides on the engineering properties of red clay. *Chinese Journal of Geotechnical Engineering, 5*, 147–156.

Ye, Q. Y. (2017). A brief discussion on the differences between red clay and expansive soil in Guangxi province. *Road Engineering, 2*, 48–50.

Yukselen-Aksoy, Y., & Kaya, A. (2011). A study of factors affecting on the zeta potential of kaolinite and quartz powder. *Environment Earth Science, 62*, 697–705.

Zhang, R. K., & Fan, G. (2003). Quantitative analytic method and experiments of X-ray diffraction period of clay minerals. *Uranium Geology, 19*, 180–185.

Zhu, Z.C., Li, J.W., Lin, F.L., Chen F., & Sun D.A. (2019). Experimental research on desorption curves of soil samples under different mineral compositions. *Chinese Journal of Geotechnical Engineering,* http://kns.cnki.net/kcms/detail/32.1124.TU.20190906.1031.020.html).

(Received 15 March 2019; revised 10 Dec 2019: AE: Yuji Arai)